

RSC Advances



This is an *Accepted Manuscript*, which has been through the Royal Society of Chemistry peer review process and has been accepted for publication.

Accepted Manuscripts are published online shortly after acceptance, before technical editing, formatting and proof reading. Using this free service, authors can make their results available to the community, in citable form, before we publish the edited article. This *Accepted Manuscript* will be replaced by the edited, formatted and paginated article as soon as this is available.

You can find more information about *Accepted Manuscripts* in the [Information for Authors](#).

Please note that technical editing may introduce minor changes to the text and/or graphics, which may alter content. The journal's standard [Terms & Conditions](#) and the [Ethical guidelines](#) still apply. In no event shall the Royal Society of Chemistry be held responsible for any errors or omissions in this *Accepted Manuscript* or any consequences arising from the use of any information it contains.

N-ethylcarbazole-Doped Fullerene as a Potential Candidate for Hydrogen Storage, Kinetics Approach

A. Mehranfar, M. Izadyar*

Department of Chemistry, Faculty of Sciences, Ferdowsi University of Mashhad, Mashhad, Iran

Abstract:

Due to the suitable possibility of the hydrogen storage applications in the liquid organic hydrogen carriers (LOHCs), a systematic analysis of the chemisorption pathway of hydrogen on N-ethylcarbazole doped fullerene (NEC@C₆₀) is given. In this study, we have investigated the nine steps of adding hydrogen onto the NEC@C₆₀ using the B3LYP/6-31G (d) level of theory in the gas phase and decalin. Based on the potential energy diagrams, Steps 5 and 9 were considered as the rate determining steps in the gas phase and decalin, respectively. Moreover, reducing the activation energy of decalin indicates solvent has an important role on the donor-acceptor interactions at the TSs. Atoms in molecules analysis confirmed the covalent nature of the C-H bonds that was formed in the TSs by potential energy densities. Comparison between the pure NEC and NEC@C₆₀ showed that the doping on the LOHCs improved the aspects of the kinetic viewpoint.

* izadyar@um.ac.ir

Keywords: Fullerene, Hydrogen storage, Kinetic, Mechanism, N-ethylcarbazole, Doping.

Introduction:

Hydrogen has been recognized as a promising source of energy. Some features, such as abundant in nature and free environmental pollution make it an ideal material as a clean energy carrier.¹ One of the most important technical challenges for practical use of hydrogen energy in large-scale applications is to find feasible and safe materials which have high gravimetric and volumetric density.²⁻¹¹

Many of nanostructured materials such as nanotubes, nanofibers and hybrid nanostructures have been proposed as materials for hydrogen storage.^{11,12} Despite much research on hydrogen uptake by carbonaceous materials, the actual mechanism of storage still remains a mystery. This mysterious nature arise of the different types of interactions, including Van der Waals, ionic and covalent interactions.¹²

The first type is based on Van der Waals attractive forces (physisorption), and in the second type, the overlap of the highest occupied molecular orbital of carbon with the occupied electronic wave function of the hydrogen electron is created with a strong chemical association (chemisorption).^{8,13,14}

Light weight and high surface-to-volume ratio of carbon nanostructures has attracted attention the hydrogen storage via these materials. Although carbon nanostructures are not ideal materials for storage at ambient thermodynamic conditions, because pristine carbon nanostructures interacting with hydrogen in the physisorbed molecular form and the binding energy of hydrogen in physisorbed state is very small at a very low temperature.¹⁵

First report on hydrogen storage in carbon nanotubes presented by Dillon et al. at 133 K.^{8,9} Their studies showed that hydrogen storage capacity of pure carbon nanotubes is not greater than 1 wt. % at ambient temperature. Also theoretical studies indicate that high hydrogen content are not achievable through physical adsorption of hydrogen in the pure carbon nanotubes.¹⁰

Fortunately, the physical and chemical properties can be modified by doped and induce defects in nanotubes. The successful synthesis of carbon nanotubes doped with nitrogen was conducted through different techniques.^{12,16} Research studies show that doped nanomaterials like nanotubes, nanofibers and nanospheres increases the binding energies at ambient temperature and pressure.^{1,17-22}

According to the ability of the double bond hydrogenation reaction, fullerene can act as a potential hydrogen storage materials. C₆₀ is a model of the zero-dimensional carbon nanostructure²³ with radius curvature of 3.55 °A which makes

it a better catalyst than the majority nanotubes.^{3,24} Also, the curved surface of the C_{60} prevents the interference groups to be adsorbed.

Structural heterogeneity in terms of chemical modification of nanostructures with nitrogen has been considered as a means to strengthen the substrate-hydrogen interaction.²⁵ Actually, aromaticity of C_{60} lead to thermodynamic stability and less reactivity. One of the ways to establish the ionic surface in C_{60} is doped suitable elements on the molecular surface. Zhang et al. studied the charged fullerene surface as a high-capacity hydrogen-storage medium.²⁶

The polyaromatic rings could be regularized the enthalpies and facilitates reversible hydrogenation via substitution of nitrogen under ambient conditions.²⁷ Some compounds such as carbazole and N-ethylcarbazole, because of the gravimetric storage capacities more than 5.5 wt. %, are potential candidates for hydrogen storage.²⁸

Pez et al. proposed organic heterocycles for the first time for usage as hydrogen storage materials at Air Products.²⁹ Their observation was published in a series of key patents.³⁰ Recently, investigate onto the hydrogenation of N-ethylcarbazole using a commercially available ruthenium catalyst has been done by Sotoodeh et al.³¹ Sotoodeh et al. determined hydrogenation of N-ethylcarbazole (NEC) at 7MPa and 150°C.³¹ Also decalin was used as the solvent in the dehydrogenation process.³²⁻³⁵

Temperature effect on hydrogen uptake onto N-ethylcarbazole was studied by Eblagon et al at 120°C- 170°C. They confirmed the reaction rate is increased via increase temperature. However, there is no significant difference in the reaction rate between 150°C and 170°C.³⁶ U.S. Department of energy (D.O.E) target for hydrogen storage are summarized in the table 1.

As previously mentioned, despite extensive research on hydrogen storage materials, the actual mechanism of storage is unknown. Here, we have tried to illustrate the kinetics and mechanism of hydrogen storage on a new proposed nanostructure of N-ethylcarbazole@C₆₀.

In order to investigate the behavior of hydrogen storage in the various conditions, we have calculated Gibbs free energy and corrected interaction energy at four different conditions to describe the NEC-doped fullerene structure:

- A. At standard conditions (0.101325MPa and 25°C) in the gas phase
- B. At 150°C and 7MPa in the gas phase.
- C. In decalin as the solvent.
- D. At 150°C and 7MPa in decalin.

Table 1. U.S. Department of energy (D.O.E.) targets for hydrogen storage systems.³⁷

Storage parameter	Units	Targets	
		2020	Ultimate

Gravimetric capacity	kWh/kg	1.8	2.5
	wt%	5.5	7.6
Volumetric capacity	kWh/L	1.3	2.3
	gH ₂ /L	40	70
H ₂ delivery temperature	°C	-40/85	-40/85
H ₂ Min delivery pressure	bar (abs)	5	3
H ₂ Max delivery pressure	bar (abs)	12	12

Computational Details:

All structures of the reactants, intermediates, transition states, and products involved in this study, were fully optimized in the gas phase using the hybrid density functional theory, B3LYP^{38,39} and 6-31G(d) basis set as implement in Gaussian09 package.³³

The energies of the structures were further improved by single-point calculations at the B3LYP/6-311++G (d,p), M062X/6-311++G (d,p) and MPWB95/6-311++G (d, p) levels of theory to achieve more accurate energy for the various structures.

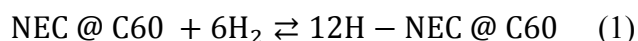
Assess the nature of the stationary points on the corresponding potential energy diagram (PED) was determined by the vibrational frequency analysis. These calculations were performed at the standard and experimental conditions (423.15 K, 7 MPa). Solvation free energy corrections were computed by the

conductor like polarizable continuum model (CPCM) calculations in decalin for consistency to the experiments.¹⁵

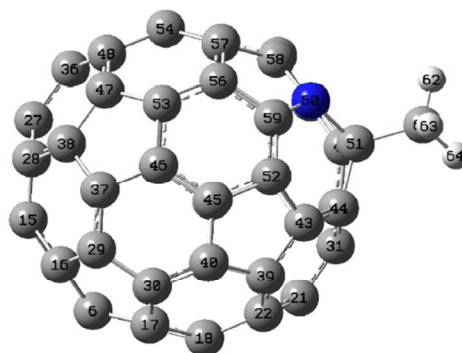
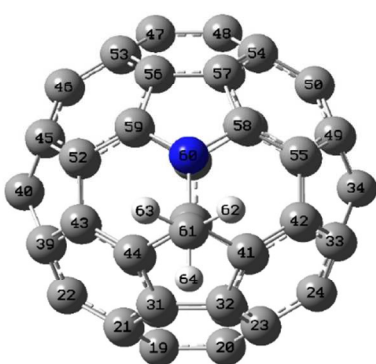
IRC (intrinsic reaction coordinate) calculations were conducted to verify the true transition states and ensure that the transition states do in fact connect the proper adjacent minima. All the calculations have been performed using Gaussian 09 packages.³² Natural bond orbital (NBO) analysis⁴⁰ was done to have knowledge of the electronic charge distribution during the hydrogen storage process. Quantum theory of atoms in molecules (QTAIM) method using AIM2000 package⁴¹ was applied for topological analysis of the electron density.

Results and Discussion:

A fullerene combines proper electronic and geometric structures. These properties of fullerenes can make it suitable to have a significant influence on the performance of the hydrogen storage mechanism. Equation 1 represents hydrogen storage reaction of NEC-doped fullerene, which we have identified as well-suited for computational study.



The optimized structure of N-ethylcarbazole doped Fullerene (NEDF) is



shown in
Figure 1.

Figure 1. Optimized structure of N-ethylcarbazole doped fullerene (NEC @ C₆₀), side and up view.

The pathway of NEC hydrogenation can be divided into eight stages:

Stages I and II: hydrogenation of NEC to dihydro-NEC, Stages III and IV: hydrogenation of dihydro-NEC to tetrahydro-NEC, Stage V: hydrogenation of tetrahydro-NEC to hexahydro-NEC, Stage VI: hydrogenation of hexahydro-NEC to octahydro-NEC, Stage VII: hydrogenation of octahydro-NEC to decahydro-NEC, Stage VIII: hydrogenation of decahydro-NEC to dodecahydro-NEC.

Also, another possible pathway has been examined in which two hydrogen molecules are added simultaneously to the reactant and this pathway found to be more favorable from the energy point of view than other ways.

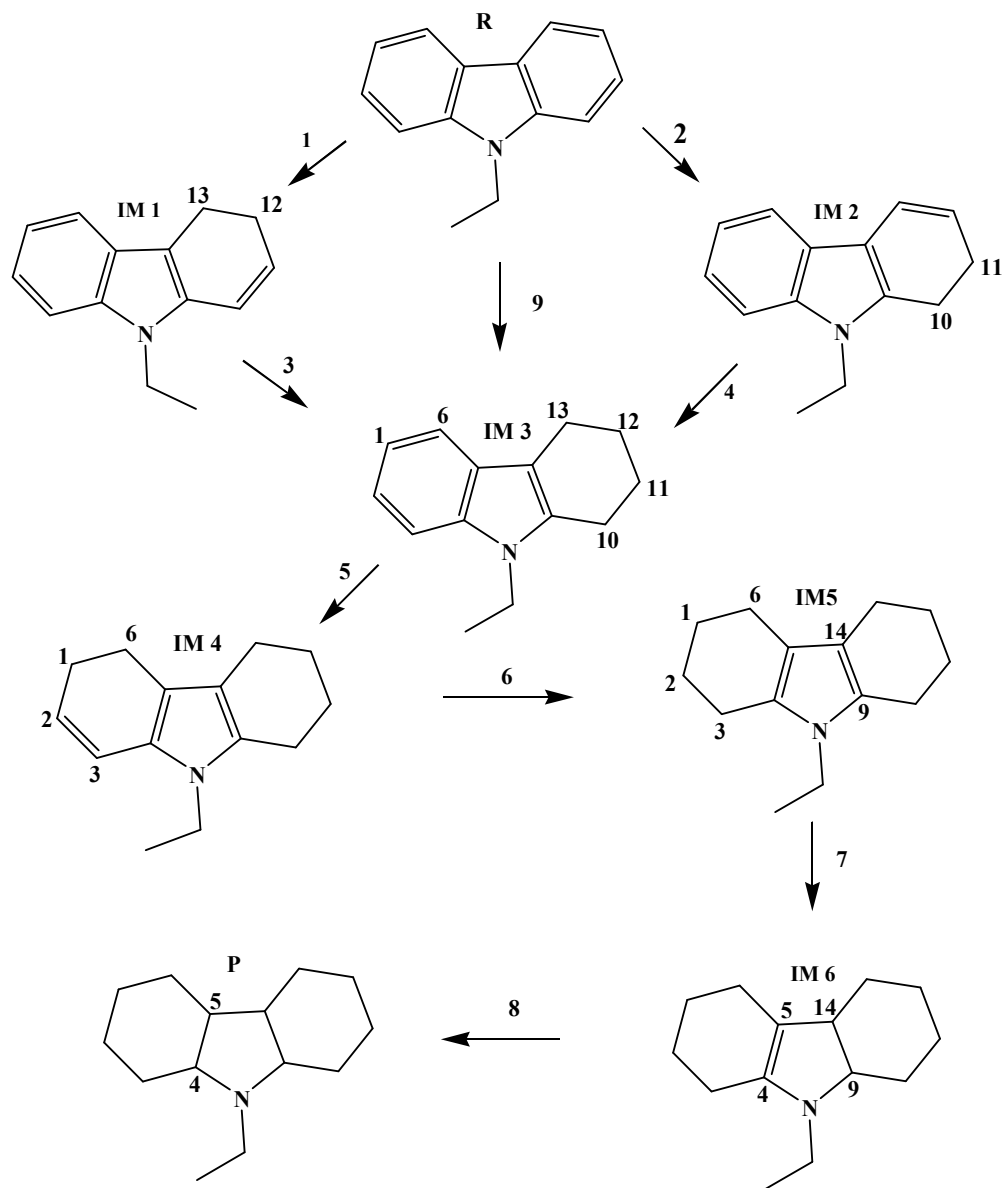
Hydrogenation in the gas phase:

Main geometrical parameters of the optimized structures in the gas phase have been evaluated during the hydrogenation process and given in Table S1. According to the Table S1, H-H bond length is increased while C-H bond length is reduced during the reaction. Scheme 1 shows the hydrogenation steps on NEC@C₆₀.

Optimized transition structures (TSs) of scheme 1 have been shown in Figure S1. The activation and thermodynamic parameters for all the studied steps

have been reported in Table 2 and compared with the experimental data of Eblagon et al.^{27,35}

Potential energy diagram of NEC@C₆₀ hydrogenation pathways in the gas phase is shown in Figure 2, blue and red colors in the standard and experimental



Scheme 1. N-ethylcarbazole hydrogenation pathways. IM1 and IM2: dihydro- N- ethylcarbazole, IM3: tetrahydro- N- ethylcarbazole, IM4: hexahydro- N- ethylcarbazole, IM5: octahydro- N- ethylcarbazole, IM6: decahydro- N- ethylcarbazole, P: dodecahydro- N- ethylcarbazole

conditions (423.15K, 7MPa), respectively. Note that we hereafter present the energetic results in the form of standard conditions [experimental conditions].

A single H₂ molecule could be adsorbed on the reactant during the paths 1 and 2. According to Figure 2, TS9 with a relative energy of 93.5 kcal.mol⁻¹ [91.6 kcal.mol⁻¹] is higher than TS1 and TS2 (Figure 2, solid line and dash line, respectively). The calculated Gibbs free energies of the reaction for paths 1 and 2 are 5.8 and 3.3 kcal.mol⁻¹, respectively. These calculated values show that these paths are not favorable ($\Delta G > 0$).

Therefore, path 9 has been considered as the first favorite pathway of the hydrogen storage, thermodynamically ($\Delta G = -15.2$ kcal.mol⁻¹). After passing through the TS9, IM 3 is formed. The activation energy for this step is 82.2 kcal.mol⁻¹ [82.5 kcal.mol⁻¹] and two hydrogen molecules are stored on NEC-doped fullerene during this step. Higher value of the relative Gibbs free energy of the TS5 (105 kcal.mol⁻¹ [105.2 kcal.mol⁻¹]) than other steps makes it the rds for the overall reaction. At this stage, three molecules of hydrogen have been saved with intake an activation energy of 97.2 kcal.mol⁻¹ [97.1 kcal.mol⁻¹].

In order to store the fourth hydrogen molecule, an activation energy of 68.8 kcal.mol⁻¹ [69.1 kcal.mol⁻¹] is needed. Gibbs free energy value of -20.5 kcal.mol⁻¹ [-20.2 kcal.mol⁻¹] for this step makes it thermodynamically favorable. Adding of the fifth and sixth hydrogen molecules due to the Gibbs energy of reaction of 14.2 kcal.mol⁻¹ [14.4 kcal.mol⁻¹] and 1.9 kcal.mol⁻¹ [2.4 kcal.mol⁻¹] is not appropriate,

thermodynamically, which request the activation energy of $67.0 \text{ kcal.mol}^{-1}$ [$66.9 \text{ kcal.mol}^{-1}$] and $64.5 \text{ kcal.mol}^{-1}$ [$64.3 \text{ kcal.mol}^{-1}$], respectively.

Comparison between the energetics of the reaction in the standard and experimental conditions does not show any meaningful description except in the activation entropy, experimental conditions reduce the entropy of transition states.

Table 3 shows the calculated Gibbs free energies in the rate determining steps for all studied paths.

Table 2. Calculated thermodynamic and activation parameters for hydrogenation of NEC@C_{60} to 12H-NEC@C_{60} in the gas phase at the standard and experimental (150°C and 7MPa) conditions.

Step NO.	$\Delta G(\text{kcal. mol}^{-1})$		$\Delta G^\ddagger(\text{kcal. mol}^{-1})$		$-\Delta S^\ddagger(\text{cal. (mol. K)}^{-1})$		$E_a(\text{kcal. mol}^{-1})$	
	Standard	Exp	Standard	Exp	Standard	Exp	Standard	Exp
1	5.8	6.0	80.9	88.1	28.5	20.5	73.5	81.1
2	3.3	3.5	79.8	80.0	29.4	22.4	72.2	72.2
3	-20.9	-20.6	76.4	76.3	27.4	19.7	69.4	69.7
4	-18.4	-18.1	72.8	72.7	27.3	19.6	65.8	66.1
5	-4.7	-4.5	105.0	105.2	29.4	22.3	97.2	97.1
6	-20.5	-20.2	75.9	75.8	28.5	19.8	68.8	69.1
7	14.2	14.4	74.8	75.1	30.1	23.2	67.0	66.9
8	1.9	2.4	72.2	72.5	29.9	23.2	64.5	64.3
9	-15.2	-14.6	93.5	91.6	41.5	25.4	82.2	82.5

Fullerene Hydrogenation out of the NEC sites

Since hydrogen molecules can be differently oriented around the fullerene, hydrogen uptake was investigated in other places on fullerene. Activation and thermodynamic parameters have been obtained from different sites of C_{60} (not NEC). Despite of decrease in activation energy through these routes (82.4 kcal.mol⁻¹), Gibbs free energy is positive (9.1 kcal.mol⁻¹), therefore they are thermodynamically unfavorable. These findings are in accordance with the previous works of the ionic center creation in the fullerene.²⁶

Verification of the selected computational method:

In order to improve the level of the theory, including more effective Van der Waals interaction, single point energy calculations were done by MPW95 and M062X using the 6-311++G (d, p) basis set. Comparison between the B3LYP and these functionals (Table 4) confirmed the rate determining step was the same, although they were numerically different.

Investigate the Table 4 proved that B3LYP/6-31G(d) level of the theory is sufficient enough for our purpose. According to the relative energies listed in Table 4, NEC@ C_{60} has less activation energy than pure NEC. This result could be interpreted by the number of π electrons which interact with hydrogen molecules.

It is worthwhile to rationalize that why $\text{NEC}@C_{60}$ is preferred than NEC to store hydrogen in this model.

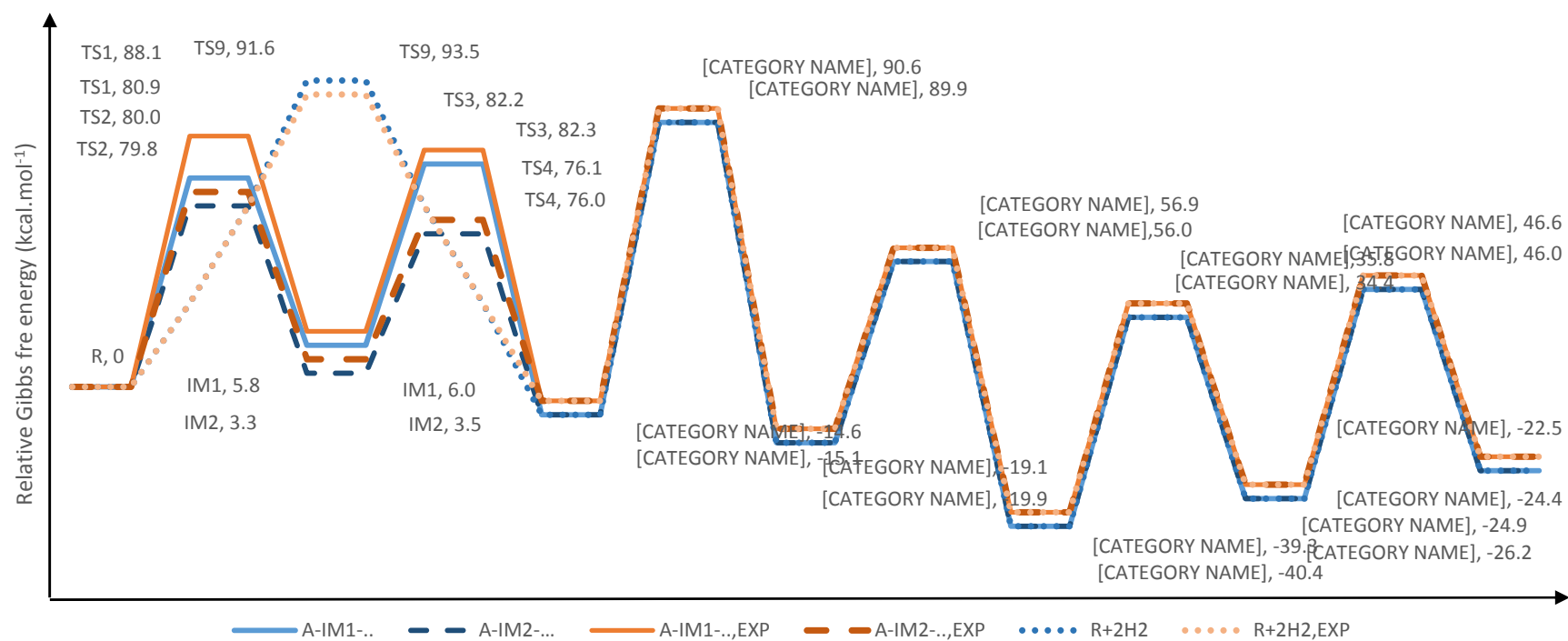


Figure 2. Potential energy diagram for the hydrogenation of NEC@C₆₀ in the gas phase, blue line: standard conditions, red line: experimental conditions (150°C, 7MPa). Solid line: NEC@C₆₀ hydrogenation through IM1, Dash line: NEC@C₆₀ hydrogenation through IM2, Dot line: NEC@C₆₀ hydrogenation through TS9.

Table 3. Calculated Gibbs free energies of the rate determining steps (rds) for all subroutes in the gas phase at the standard and experimental conditions.

Path R–P, Gas phase	Steps of subroutes	$\Delta G^{\ddagger}_{\text{rds}}$ (kcal. mol ⁻¹)
Standard conditions	R,TS1,IM1,TS3,IM3,TS5,IM4,TS6,IM5,TS7,IM6,TS8,P	105.0
	R,TS2,IM2,TS4,IM3,TS5,IM4,TS6,IM5,TS7,IM6,TS8,P	105.0
	R,TS9,IM3,TS5,IM4,TS6,IM5,TS7,IM6,TS8,P	105.0
Experimental conditions	R,TS1,IM1,TS3,IM3,TS5,IM4,TS6,IM5,TS7,IM6,TS8,P	105.2
	R,TS2,IM2,TS4,IM3,TS5,IM4,TS6,IM5,TS7,IM6,TS8,P	105.2
	R,TS9,IM3,TS5,IM4,TS6,IM5,TS7,IM6,TS8,P	105.2

Hydrogenation in decalin

Conductor like polarizable-continuum model (CPCM) was applied to investigate the effect of decalin as the solvent on the rate of hydrogen storage via NEC@C₆₀. Main geometrical parameters in decalin were reported in Table S2. H–H bond length is increased from 0.74 Å to 1.42 Å during the reaction. Average lengths of C–C and C–H bonds are 1.51 Å and 1.81 Å at the TSs, respectively. Comparison of changes in the bond length at the TSs shows that hydrogen storage happens through a non-synchronous concerted mechanism.

Calculated thermodynamic and activation energies for all species have been reported in the Table 5. Potential energy diagrams of the hydrogen storage reaction in the presence of decalin at the standards and experimental conditions were shown in Figure 3 in blue and red colors, respectively.

Similar to the gas phase, thermodynamic and kinetic parameters in decalin suggests that step 9, with an activation energy of 81.25 kcal.mol⁻¹ [81.65 kcal.mol⁻¹], is rds. Investigate the thermodynamic and kinetic parameters obtained in

experimental conditions reveals reduction in the entropy of activation and an increase in the Gibbs free energy, however it has no significant effect on the activation energy. Gibbs free energy for the rate determining steps in all studied paths in decalin are shown in Table 6.

Table 4. Relative Energies (in kcal.mol⁻¹) for the TSs of NEC and NEC doped C₆₀ in the gas phase at the MPWB95, M062X and B3LYP by 6-311++G (d, p) basis set.

Step NO.	MPWB95		M062X		B3LYP		
	NEC@C ₆₀	NEC	NEC@C ₆₀	NEC	NEC@C ₆₀	NEC	NEC@C ₆₀ (6-31G(d))
Step 1	63.63	95.88	75.50	105.21	72.18	124.81	71.03
Step 2	68.65	92.50	73.55	102.23	73.20	101.45	60.70
Step 3	58.67	72.47	77.44	91.65	68.84	82.71	68.41
Step 4	56.78	72.46	72.23	88.98	64.61	81.83	64.43
Step 5	87.08	88.63	98.37	97.12	95.75	97.22	94.93
Step 6	61.19	68.82	75.23	88.17	68.28	79.08	67.57
Step 7	60.48	76.86	65.93	80.72	63.83	80.45	62.25
Step 8	55.19	80.05	61.74	86.73	62.98	84.37	46.12
Step 9	68.21	50.78	73.45	60.35	75.73	58.58	76.76

Comparison between the results of the NEC@C₆₀ hydrogenation with NEC storage systems⁴⁵ confirms that the doping NEC on fullerene in the presence of decalin improves the reaction rate by decrease in the activation energy of rds.

Table 5. Calculated thermodynamic and activation parameters of the hydrogenation reaction in decalin at

standard and experimental conditions (150°C and 7MPa).

Step NO.	$\Delta G(\text{kcal. mol}^{-1})$		$\Delta G^\ddagger(\text{kcal. mol}^{-1})$		$-\Delta S^\ddagger(\text{cal. (mol. K)}^{-1})$		$E_a(\text{kcal. mol}^{-1})$	
	Standard	Exp	Standard	Exp	Standard	Exp	Standard	Exp
1	5.0	5.7	86.9	86.6	28.5	20.8	79.6	79.8
2	2.7	2.9	96.0	96.2	29.2	21.9	89.0	88.6
3	-21.4	-21.0	75.1	74.7	24.7	16.8	68.9	69.2
4	-18.5	-18.0	70.0	69.8	26.9	19.2	63.1	63.3
5	-4.8	-4.6	78.3	78.4	28.5	20.9	71.0	71.2
6	-20.6	-20.3	73.1	73.0	27.3	19.5	66.1	66.4
7	14.0	14.3	89.8	89.8	28.6	21.0	82.4	82.6
8	1.5	2.0	72.0	72.2	29.8	23.1	64.2	64.1
9	-15.8	-15.3	92.6	90.7	25.4	41.9	81.2	81.6

Population analysis

Further examination was conducted by natural bond orbital (NBO) calculations. This study of the structures translates the complex quantum-mechanical wave function into a more tangible Lewis dot like formalism (natural Lewis structure). This mixing of the donor and acceptor orbitals can be solved by the second order perturbation theory. This technique leads to an overall energy lowering, stabilization and a quantum mechanical phenomenon.^{42,43}

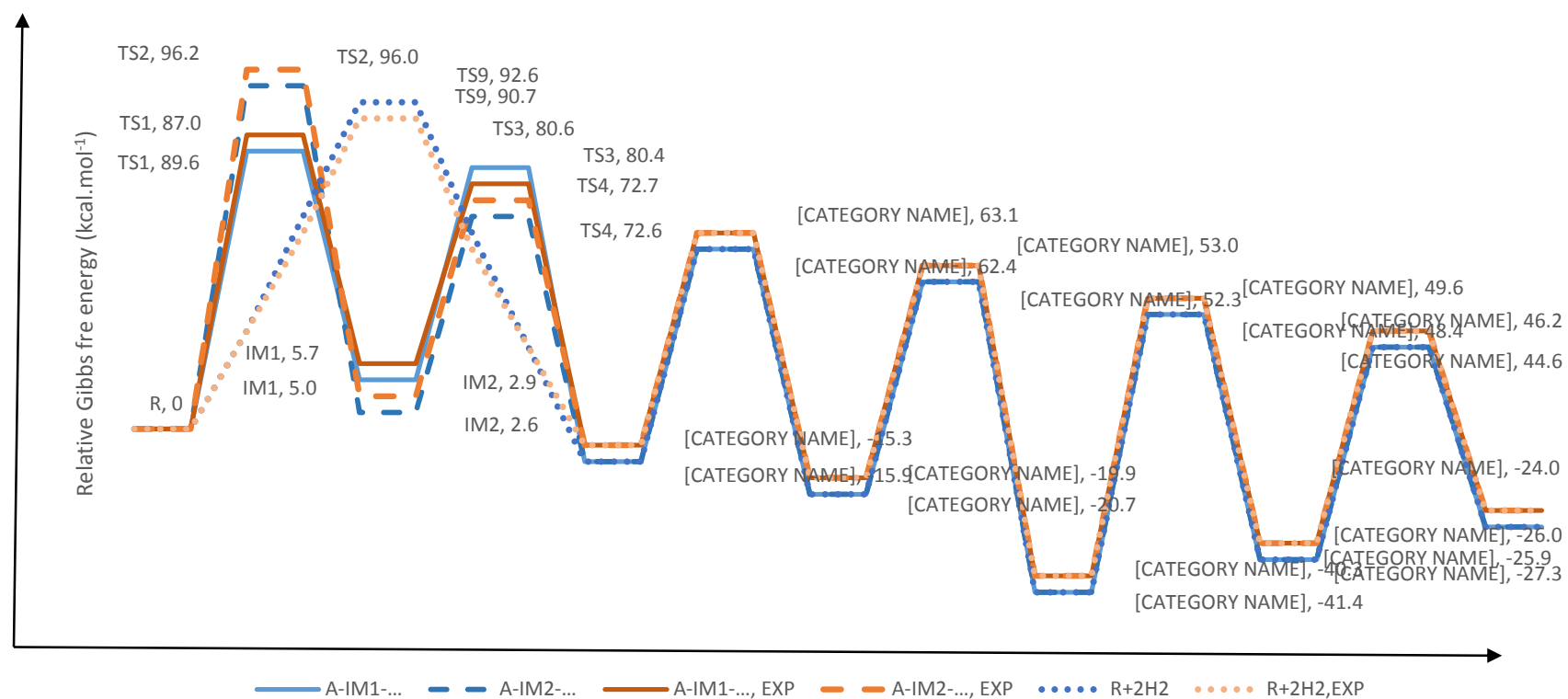


Figure 3. Calculated relative Gibbs free energies for the hydrogenation of NEC@C₆₀ in decalin, blue line: standard conditions, red line: experimental conditions (150°C, 7MPa). Solid line: NEC@C₆₀ hydrogenation through IM1 formation, Dash line: NEC@C₆₀ hydrogenation through IM2 formation, Dot line: C₆₀H₃N hydrogenation through TS9.

Table 6. Calculated Gibbs free energies for the rate determining steps (rds) of all sub routes in decalin at the standard and experimental conditions.

Path R-P, Decalin	Steps of the subroutes	$\Delta G^{\ddagger}_{\text{rds}}$ (kcal. mol ⁻¹)
Standard conditions	R,TS1,IM1,TS3,IM3,TS5,IM4,TS6,IM5,TS7,IM6,TS8,P	78.3
	R,TS2,IM2,TS4,IM3,TS5,IM4,TS6,IM5,TS7,IM6,TS8,P	78.3
	R,TS9,IM3,TS5,IM4,TS6,IM5,TS7,IM6,TS8,P	92.6
Experimental conditions	R,TS1,IM1,TS3,IM3,TS5,IM4,TS6,IM5,TS7,IM6,TS8,P	78.4
	R,TS2,IM2,TS4,IM3,TS5,IM4,TS6,IM5,TS7,IM6,TS8,P	78.4
	R,TS9,IM3,TS5,IM4,TS6,IM5,TS7,IM6,TS8,P	90.7

Significant donor–acceptor interactions were calculated and reported in Table S3. According to the table, the sp^2 bonded carbons serve as hydrogen acceptors at the center of the store. The most important transfers are transferring between a bonding pair of H (BP_{H68}) and anti-bonding orbital of C-H ($\sigma_{C50-H68}^*$) at the TS4 with an energy of 66.81 kcal.mol⁻¹ in the gas phase, which reduce to 44.26 kcal.mol⁻¹ in decalin.

Also at the TS5, we observed large stabilizing effect is due to strong orbital interactions between the bonding and anti-bonding orbitals of C-C ($\pi_{C46-C53}$, $\pi_{C46-C53}^*$) and the anti-bonding orbitals of H-H ($\sigma_{H69-H70}^*$) are 11.24 and 17.26 kcal.mol⁻¹, respectively. The strongest delocalization interaction is related to the $\sigma_{H67-H68}^*$ to LP_{C52} (93.18 kcal.mol⁻¹) and $\sigma_{H67-H68}^*$ to $\pi_{C52-C59}^*$ (13.80 kcal.mol⁻¹) is observed at the TS6 in the gas phase. In the case of TS8, the interaction of $\pi_{C56-C59}^*$ to $\sigma_{H71-H72}^*$ (19.82 kcal.mol⁻¹) in the gas phase is increased to 20.73 kcal.mol⁻¹ in decalin.

Overall, the values of E(2) of the bonds involved in the hydrogenation process to adjacent bonds decreased at the transition states. Moreover, the emergence of new transitions represents that transitions are done to bond formation and hydrogenation reaction.

Electronic atomic charges for the atoms are shown in Table S4 at the center of hydrogen store. Charge analysis shows that partial charges are transferred from the H2 to the NEC@C₆₀. Assessment of this analysis of the rate determining step (Step 5)

show that the partial charge on the hydrogen atoms from about 0 e (IM3) is changed to 0.053 e (gas phase) and -0.042 e (decalin) at the TS5. The corresponding changes for carbon atoms involved in the hydrogen storage are from -0.029 e and 0.004 e to 0.019 e and -0.134 e in the gas phase and decalin, respectively.

In decalin, hydrogen atoms with partial charge of 0 e are added to carbon atoms with atomic charges of 0.011 e, -0.027 e, 0.008 e and -0.066 e at the rds (Step 9). Also, changes of atomic charge for hydrogen atoms are -0.005 e, 0.003 e, 0.431 e and 0.282 e, while for carbon atoms are -0.230 e, -0.181 e, 0.057 e and -0.174 e.

Natural electron configurations are shown in Table S5. Natural electron configurations of the hydrogen and carbon atoms involved in the center of the reaction have been changed at the rds in the gas phase (Step5). The corresponding changes for the TS9 in decalin confirmed the interactions between carbon and hydrogen atoms during the C-H bond formation and achieving effective hydrogen storage.

The Population analysis shows that N atom acts as an electron acceptor and carbon atoms of the C–N bonds are donors. While at TSs, when C–H bonds are formed, carbon atoms acts as the acceptor and hydrogen atoms are donors. These findings were shown in figures S2 and S3.

QTAIM analysis

QTAIM studies were used for the analysis of the topological parameters such as electron density (ρ), Laplacian ($\nabla^2\rho$), kinetic (G), and potential (U) electronic energy density of the bond critical points of C-H⁴⁴ and reported in Table 7.

Positive values of electron density at the TSs confirmed the existence of the proper C–H bond interaction. Higher values of electron density of the TS5 show the solvent effect on the stabilizing of the rds and charge transfers in decalin, but in the case of TS9, solvent shows different action. This means that electron density is increased for one of the C-H bonds at the TS9 in decalin, which is in contrast to the other C-H bond. But considering the Laplacian and G/U values confirmed that the second C-H bond (last line in table 7) shows the better interaction with higher covalent characters.

Comparison between the calculated ratios of G/U confirmed a covalent nature of the carbon and hydrogen atom interactions at the TSs 5 and 9. This character is larger in the case of TS9 and shows the solvent effects on the stability of the TS.

Dehydrogenation process

Similar to the hydrogen storage, the process of hydrogen release is important, too. The proposed mechanism for the hydrogen release is the reverse of the mechanism shown in scheme 1. Therefore, the transitions states from the dehydrogenation process is the same of the transitions states in which the activation energies of the backward reactions are important (E_{a_b}). The activation and thermodynamic parameters in all

studied conditions for the mechanism of hydrogen release are calculated and reported in table 8.

Table 7. Properties of electron density, Laplacian and kinetic (G) to potential (U) electronic energy density ratio (in au.), G/U , for the BCPs of C-H bonds at the TSs.

Step NO.	$\rho(r)$		$L(r)$		G/U	
	Gas phase	Decalin	Gas phase	Decalin	Gas phase	Decalin
1	0.192	0.222	0.115	0.155	0.155	0.157
2	0.131	0.155	0.552	0.028	0.182	0.401
3	0.125	0.168	0.028	0.066	0.375	0.284
4	0.198	0.218	0.113	0.150	0.206	0.166
5	0.074	0.241	-0.031	0.183	0.696	0.133
6	0.146	0.146	0.040	0.118	0.343	0.199
7	0.280	0.246	0.235	0.202	0.129	0.128
8	0.061	0.059	-0.021	-0.012	0.701	0.758
9- Synchronous	0.093	0.028	0.015	-0.026	0.364	0.908
addition of 2H ₂	0.127	0.146	0.027	0.040	0.374	0.354

According to table, hydrogen removal from the five-membered ring is favorable, thermodynamically. These results are in accordance with the experimental results obtained for the NEC dehydrogenation.^{28,31,32} Actually, the participation of the heteroatom reduces the energy barrier of the five-membered ring.

Table 8 shows the lowest value of the activation energies when P and IM6 act as the reactants in the dehydrogenation process. Moreover, IM1→R and IM2→R paths

with the negative Gibbs free energy of the reaction are thermodynamically favorable, because their products have greater aromaticity and stability. These steps are rds in dehydrogenation process due to the highest value of the activation energies.

Table 8. Calculated thermodynamic and activation parameters for dehydrogenation of 12H-NEC@C₆₀ to NEC@C₆₀ in the gas phase and decalin phase at the standard and experimental (150°C and 7MPa) conditions.

path	$\Delta G(\text{kcal. mol}^{-1})$				$E_a(\text{kcal. mol}^{-1})$			
	Gas phase		Decalin		Gas phase		Decalin	
	Standard	Exp	Standard	Exp	Standard	Exp	Standard	Exp
P→IM6	-1.9	-2.4	-1.5	-2.0	72.0	72.6	72.2	72.8
IM6→IM5	-14.2	-14.4	-14.0	-14.3	61.8	62.3	77.4	78.1
IM5→IM4	20.5	20.2	20.6	20.3	98.3	99.2	95.8	96.7
IM4→IM3	4.7	4.5	4.8	4.6	111.1	111.6	84.8	85.5
IM3→IM2	18.4	18.1	18.5	18.0	93.3	94.1	90.7	91.6
IM3→IM1	20.9	20.6	21.4	21.0	99.4	100.3	99.4	100.3
IM2→R	-3.3	-3.5	-2.7	-2.9	77.8	78.4	94.7	95.4
IM1→R	-5.8	-6.0	-5.0	-5.7	76.6	84.7	83.0	83.7
IM3→R	15.2	14.6	15.9	15.3	115.2	116.8	115.1	116.6

Conclusion

In this article, we have introduced NEC@C₆₀ systems as a new hydrogen storage material and investigated the mechanism of hydrogenation on NEC@C₆₀ systems through the quantum chemistry approach.

The gravimetric storage of NEC@C₆₀ is about 1.5-2 wt% which is less than the gravimetric storage on NEC (more than 5.5 wt%). But finding the materials that meet all the criteria for hydrogen storage is very difficult. In this study, our focus is on the improving the kinetics of hydrogen storage not gravimetric preferences. Transition states were evaluated through the structure and energetic properties in addition to the vibrational frequency analysis. According to the activation parameters, the fifth step of the hydrogen storage is the rate determining step in the gas phase. However, in the presence of decalin as the solvent, the rds is changed to the ninth step. Comparison of the activation energies of NEC@C₆₀ in the gas phase and decalin shows that the hydrogenation barrier in decalin is smaller. These quantitative observations are consistent with NBO analysis, our observations show that N atom acts as an acceptor while H atom is a donor. QTAIM data confirm that C–H bonds are covalent in nature and hydrogen storage is a chemisorption process on NEC@C₆₀.

Thermodynamic parameters and kinetic studies demonstrated that the dehydrogenation process started from the five-membered ring. This study gets good kinetic approach to improve the rate of hydrogen storage on NEC. The results show that fullerene in the decalin solvent can increase the rate of hydrogenation reaction of NEC.

From the obtained results, it can be predicted easily that create similar doping on all the fullerene surface can be increased storage gravimetric capacity along with improve in the kinetics of the hydrogen storage capacity. Finally, we believe that the results of this work would be valuable for the understanding of the mechanisms of hydrogen storage using NEC@C₆₀ as new material.

Acknowledgements

Research Council of Ferdowsi University of Mashhad is gratefully acknowledged for the financial support of this work (Grant No. 3/29590, 1392/10/07). We hereby acknowledge that part of this computation was performed on the HPC center and the Seismology center of Ferdowsi University of Mashhad.

References

1. L. Xu, Q. Ge, *Int. J. Hydrogen Energy.*, 2013, 38, 3670-3680.
2. M. Li, Y. Li, Z. Zhou, P. Shen, Z. Chen, *Nano. Lett.*, 2009, 9, 1944-1948.
3. P. A. Berseth, A. G. Harter, R. Zidan, A. Blomqvist, C. M. Araujo, R. H. Scheicher, R. Ahuja, P. Jena, *Nano. Lett.*, 2009, 9, 1501-1505.
4. S .Bhattacharya, C .Majumder, G. P. Das, *Bull. Mater. Sci.*, 2009, 32, 353-360.

5. T. Yildirim, S. Ciraci, *Phys. Rev. Lett.*, 2005, 94, 1755011-1755014.
6. Q. Sun, Q. Wang, P. Jena, Y. Kawazoe, *J. Am. Chem. Soc.*, 2005, 127, 14582-14583.
7. P. O. Krasnov, F. Ding, A. K. Singh, B. I. Yakobson, *J. Phys. Chem. C.*, 2007, 111, 17977- 17980.
8. M. U. Niemann, S. S. Srinivasan, A. R. Phani, A. Kumar, D. Y. Goswami, E. K. Stefanakos, *J. Nanomater.*, 2008, 1-9.
9. Z. Liu, Q. Xue, C. Ling, Z. Yan, J. Zheng, *Comp. Mater. Sci.*, 2013, 68, 121-126.
10. E. Durgun, S. Ciraci, T. Yildirim, *Phys. Rev. B.*, 2008, 77, 0854051-0854059.
11. C. Liu, F. Li, L. P. Ma, H. M. Cheng, *Adv. Mater.*, 2010, 22, E28–E62.
12. Q. Sun, Q. Wang, P. Jena, Y. Kawazoe, *J. Am. Chem. Soc.*, 2005, 127, 14582-14583.
13. A. Nikitin, X. Li, Z. Zhang, H. Ogasawara, H. Dai, A. Nilsson, *Nano. Lett.*, 2008, 8, 162-167.
14. M. Dixit, T. A. Maark, S. Pa, Sweden, India.
15. Y. Li, G. Zhao, C. Liu, Y. Wang, J. Sun, Y. Gu, Y. Wang, Z. Zeng, *Int. J. Hydrogen Energy.*, 2012, 37, 5754-5761.
16. M. Mananghaya, E. Rodulfo, G. N. Santos, *Int. J. Sci. Eng. Res.*, 2012, 3, 1-7.
17. B. J. Kim, Y. S. Lee, S. J. Park. *Int. J. Hydrogen Energy.*, 2008, 33, 4112-4115.
18. L. Zubizarreta, J. Menndez, J. Pis, A. Arenillas, *Int. J. Hydrogen Energy.*, 2009, 34, 3070-3076.
19. Y. Zhao, Y. H. Kim, A. C. Dillon, M. J. Heben, S. B. Zhang, *Phys. Rev. Lett.*, 2005, 94, 15550.
20. Y. Suttisawat, P. Rangsunvigit, B. Kitiyanan, M. Williams, P. Ndungu, M. Lototsky, A. Nechaev, V. Linkov, S. Kulprathipanja, *Int. J. Hydrogen Energy.*, 2009, 34, 6669-6675.

21. J. Sun, W. C. Lu, W. Zhang, L. Z. Zhao, Z. S. Li, C. C. Sun, *Inorg. Chem.* 2008, 47, 2274-2279.
22. J. Chen, F. Wu, *Appl. Phys. A.*, 2004, 78, 989-994.
23. P. Ruffieux, O. Groauning, M. Biemann, P. Mauron, L. Schlapbach, *Phys. Rev. B.*, 2002, 66, 2454161-2454168.
24. D. Saha, S. Deng, *Langmuir.*, 2011, 27, 6780-6786.
25. A. Gotzias, E. Tylianaki, S. G. Froudakis, T. Steriotis, *Micropor. Mesopor. Mat.*, 2012, 154, 38-44.
26. K. Srinivasu, K. R. S. Chandrakumar, S. K. Ghosh, *ChemPhysChem.*, 2009, 10, 427-435.
27. K. Eblagon, K. Tam, K. Yu, S. Zhao, X. Gong, H. He, L. Ye, L. Wang, A. Ramirez-Cuesta, S. Tsang, *J. Phys. Chem. C.*, 2010, 114, 9720-9730.
28. F. Sotoodeh, B. J. M. Huber, K. J. Smith, *Int. J. Hydrogen Energy.*, 2012, 37, 2715-2722.
29. R. H. Crabtree, *Energy. Environ. Sci.*, 2008, 1, 134-138.
30. G. P. Pez, et al. *International Patent WO/2005/000457*, 2005.
31. F. Sotoodeh, K. J. Smith, *Can. J. Chem. Eng.*, 2013, 91, 1477-1490.
32. F. Sotoodeh, K. J. Smith, *J. Catal.*, 2011, 279, 36-47.
33. M. J. Frisch, G. W. Trucks, H. B. Schlegel, G. E. Scuseria, M. A. Robb, J. R. Cheeseman, J. A. Montgomery, T. Vreven, K. N. Kudin, J. C. Burant, J. M. Millam, S. S. Iyengar, J. Tomasi, V. Barone, B. Mennucci, M. Cossi, G. Scalmani, N. Rega, G. A. Petersson, H. Nakatsuji, M. Hada, M. Ehara, K. Toyota, R. Fukuda, J. Hasegawa, M. Ishida, T. Nakajima, Y. Honda, O. Kitao, H. Nakai, M. Klene, X. Li, J. E. Knox, H. P. Hratchian, J. B. Cross, C. Adamo, J. Jaramillo, R. Gomperts, R. E. Stratmann, O. Yazyev, A. J. Austin, R. Cammi, C. Pomelli, J. W. Ochterski, P. Y. Ayala, K. Morokuma, G. A. Voth, P. Salvador, J. J. Dannenberg, V. G. Zakrzewski, S. Dapprich, A. D. Daniels, M. C. Strain, O. Farkas, D. K. Malick, A. D. Rabuck, K. Raghavachari, J. B. Foresman, J. V. Ortiz, Q. Cui,

A. G. Baboul, S. Clifford, J. Cioslowski, B. B. Stefanov, G. Liu, A. Liashenko, P. Piskorz, I. Komaromi, R. L. Martin, D. J. Fox, T. Keith, M. A. Al-Laham, C. Y. Peng, A. Nanayakkara, M. Challacombe, P. M. W. Gill, B. Johnson, W. Chen, M. W. Wong, C. Gonzalez, J. A. Pople, Gaussian 09, Revision B.09. Wallingford CT: Gaussian, Inc; 2009.

34. X. Ye, Y. An, G. Xu, *J. Alloys. Compd.*, 2011, 509, 152-156.

35. D. Teichmann, W. Arlt, P. Wasserscheid, *Int. J. Hydrogen Energy.*, 2012, 37, 18118-18132.

36. K. M. Eblagon, D. Rentsch, O. Friedrichs, A. Remhof, A. Zuettel, A. J. Ramirez-Cuesta, S. Tsang, *Int. J. Hydrogen Energy.*, 2010, 35, 11609-11621.

37. U.S. Department of Energy, <http://www.Eere.Energy.gov/> Technical Plan — Storage.

38. A. D. Becke, *J. Chem. Phys.*, 1993, 98, 5648-5652.

39. C. Lee, W. Yang, R. G. Parr, *Phys. Rev. B.*, 1988, 37, 785-789.

40. G. N. Lewis, *J. Am. Chem. Soc.*, 1916, 38, 762-785

41. R. F. W. Bader. AIM 2000 Program. McMaster University: Hamilton; 2000.

42. Z. M. Qian, M. S. L. Hudson, H. Raghubanshi, R. H. Scheicher, B. Pathak, C. M. Araujo, A. Blomqvist, B. Johansson, O. N. Srivastava, R. Ahuja, *J. Phys. Chem. C.*, 2012, 116, 10861-10866.

43. P. O. Löwdin, *Phys. Rev.*, 1955, 97, 1474-1489.

44. R. F. W. Bader. *Atoms in molecules: a quantum theory*. New York: Oxford University. 1990.

45. A. Mehranfar, M. Izadyar, A.A. Esmaili, *Int. J. Hydrogen Energy*, 2015, 40, 5797-5806.